Chall. Nano Micro Scale Sci. Tech., 9(2):109-116, Summer and Autumn 2021
DOI: 10.22111/CNMST.2022.39120.1215

ORIGINAL RESEARCH PAPER

Stability of Nanofluid-Surfactants as Volumetric Receivers in Parabolic Trough Solar Collectors; a Molecular Dynamic Approach

Hamed Farzaneh[1,*], Amin Behzadmehr[1], Abdolreza Samimi[2]

[1]Mechanical Engineering Department, University of Sistan and Baluchestan
[2]Chemical Engineering Department, University of Sistan and Baluchestan

Received 4 July 2021; revised 8 March 2022; accepted 12 March 2022;

ABSTRACT: Recently, using volumetric receivers as a novel idea to collect solar energy was considered. Solar radiation volumetrically absorbers with a heat transfer fluid which flows through a transparent tube. Nanofluids as working fluids were proposed by different researchers because of their interesting absorption coefficient as well as an important heat transfer coefficient. However, conditions such as the severe temperature gradient in absorber tubes and high temperature of working heat transfer fluid, deteriorate stability of the nanofluids. Considering the kinetic energy of nanoparticles, DLVO potential energy and steric repulsion between nanoparticles, a molecular approach is adopted to investigate the nanofluid stability for different nanofluids with polymeric surfactants and different operational conditions. Two types of polymeric surfactants were considered and stability diagrams introduced to show the conditions for which a nanofluid would be stable. In the case of using PAA for a given temperature gradient, increasing the working fluid temperature required smaller nanoparticle diameters to result in a stable nanofluid (nanoparticles up to 13.2 nm diameter) and for PMAA, a stable nanofluid can be achieved with larger nanoparticle diameters (about 80nm) while increasing the working fluid temperature.

KEYWORDS: *dispersion stability; DLVO; nanofluid; polymeric surfactant; volumetric receiver*

INTRODUCTION

The growing need for energy resources and reduction of conventional fossil energy sources on the one hand, and environmental hazards resulting from the use of such sources on the other hand, have made the undeniable importance of using renewable energy obvious. In the meantime, it seems that utilizing solar energy is among the promising resources that are applicable to both small and large scales. Due to the low energy density of the Sun at the ground level, concentrating solar collectors are important parts in solar power plants that convert solar energy into electrical energy. In these collectors, solar radiation from reflected surfaces is focused on the outer surface of a tubular receiver that generates significant heating energy. The latter contains heat transfer fluid flowing through the tubular receiver and its temperature increases. Improving the optical properties of the absorbent surfaces exposed to the concentrated sun's rays are among the most important results in recent decades, which resulted in solar selective surfaces. These surfaces have both a high absorption coefficient and low emissivity [2]. High absorption coefficient causes more absorption of energy while the effective area of heat transfer in this kind of surfaces is limited. Hence, the latter limits the rate of heat transfer to the working fluid and consequently the absorbent surface temperature significantly increases thereby drastically augmenting the heat losses through emission.

*Corresponding Author Email: *hamed.farzaneh@yahoo.com*
Tel.: +989366133253; Note. This manuscript was submitted on July 4, 2021; approved on March 8.

In 1970 it was found that a large temperature difference between absorbent wall and heat transfer fluid exists and the idea of using volumetric receivers containing small particles was proposed by Abdelrahman [3] and Hunt [1] for the first time. Abdelrahman showed that temperature difference between the small particles and the heat transfer fluid, due to the high surface to volume ratio of the particles, is not significant and can be ignored. In 1978, Drotning et al [4] conducted an experimental investigation on molten salts containing oxide particles to obtain their optical properties. Kumar & Tien [5] investigated molten salt flow containing small particles as volumetric receivers. Later, Lenert [2] and Lenert et al. [6] conducted numerical and experimental research to investigate the efficiency of volumetric receivers containing nanofluids. Their work provides visions as to how nanofluids can be best utilized as volumetric receivers such as in high concentration solar thermal energy conversion systems. Tyagi et al [7] theoretically studied the effect of using nanofluid in a direct absorption solar collector. They showed that the absorption of incident radiation is augmented more than nine times over that of pure water by using nanofluid. The optical properties and the feasibility of applying nanofluids in solar collectors have been studied by [8-12]. Qunzhi Zhu et al. [13] who investigated the radiative properties of nanofluids for absorption of solar radiation. Recently, solar energy absorption by the volumetric receiver systems containing nanofluids was studied by Khullar et al [14] In all these studies researchers believe that using volumetric receiver

Nomenclature

C	concentration (vol.%)
Cp	specific heat at constant pressure (J/kg.K)
D	diameter (mm)
h	heat transfer coefficient (W/m^2.K)
h_x	local heat transfer coefficient (W/m^2.K)
K	thermal conductivity
l	liter
L	level
m	number of experiments
$MAPE$	mean absolute percentage error
n	number of repetitions
Nu	Nusselt number
P	percent of contribution
Pr	Prandtl number
PC	personal computer
PID	proportional–integral–derivative
PVC	polyvinyl chloride
Q	nanofluid flow rate, (l/min)
Re	Reynolds number
T	temperature, (°C)
V	variance
Y	value of results
$\bar{Y}$	average value of results

Greek Letters

μ	viscosity (mPa.s)
ρ	density (kg/m^3)

Subscripts

bf	base fluid
Er	error
F	factor
nf	nanofluid
P	particle

systems instead of surface absorption systems can increase the efficiency of solar collectors.

However, there are many serious problems that must first be overcome prior to any application of nanofluids. Among them are the aggregation and sedimentation of nanoparticles' as well as the physicochemical stability of nanofluids being the most important issues that must be well addressed prior to any application. Sedimentation of nanoparticles causes severe problems on the hydrothermal behaviors of a process. However, various methods have been proposed for stabilization of nanofluid such as applying ultrasonic waves for breaking nanoparticle aggregates, coating nanoparticles with polymeric surfactants to prevent aggregation, external force field employment on nanofluid as well as changing of electrostatic properties of nanoparticles' surfaces by variation of PH. Although, some of these methods are effective on the stabilization of nanofluids to some extent, none of them can perfectly solve the problem of nanofluid stability. It is well known that the interparticle forces in nanofluids play an important role in nanofluid stability. In 2016, Behzadmehr et al. [15] proposed stability diagrams for nanofluid at different thermophysical conditions without any surfactants. They studied a molecular dynamic approach by considering different forces to establish stable nanofluid conditions. In 2019, Zareei et al.[16] investigated the colloidal behavior of nanoparticles in Al2o3-water nanofluid where they studied the influence of pH, surfactants and ionic strength. They concluded that the best nanofluid stability occurred at pH 4 with anionic surfactants. Cacua et al.[17] investigated the stability of Al2o3-water nanofluid. They studied the effect of CTAB and SDBS surfactants concentration on the zeta potential at different pH values and showed that SDBS at critical micelle concentration (0.064 wt.%) had the best dispersion stability. Ouikhalfan et al.[18] investigated the stability of TiO2-water nanofluid by two kinds of surfactants: CTAB and SDS. They presented that modified TiO2-water nanofluid with a volume fraction of 1.25% remains stable up to two weeks. Kaggwa et al.[19] investigated the effect of surfactants on the stability of nanofluids that can be used as working fluid in heat transfer systems. Their results revealed that C-water and CuO-water nanofluids with the Arabinogalactan (ARB) surfactant would be stable for more than 20 days compared to CTAB, SDS and SDBS surfactants. Zhai et al.[20] studied the stability of Al2O3-ethylene glycol nanofluid with PVP and SDS surfactants. Their results showed that nanofluids with PVP surfactant had the highest stability due to polymeric chain interactions.

In 2020, sharaf et al. [21] studied the Colloidal and Chemical Stability of Solar Nanofluids. They introduced some recommendations regarding current knowledge gaps in order to overcome the stability limitations hindering the deployment of solar nanofluids in practical solar applications. Razavi et al. [22] conducted an Experimental investigation on the stability and thermophysical properties of some water based nanofluids. They studied the effect of adding three different surfactants on the sedimentation of nanoparticles and showed that Surfactants of SDS, SDBS, and HCTAB with the surfactant content ratios of 1–10 had the best performance in the stability improvement of the nanofluids. Mukesh Kumar et al. [23] investigated Stability of hybrid/water nanofluids. They studied the Al2O3–Sio2/water nanofluid and showed that 0.6 wt% nanofluids has good stability. As mentioned, these researchers have tried to prepare a homogenous and stable nanofluid to be used as a working fluid. Their attempts on nanofluid stabilization were limited to amplifying the zeta potential layer around the nanoparticles. Furthermore, in some cases experimental works were carried out on breaking aggregated particles down to smaller ones.

In the author's knowledge, there had not been any attempt made to show and to present the conditions for which a nanofluid would be stable and the nanoparticle aggregation does not occur throughout the process cycle.

Thus, it is very important to have a new idea and a good understanding of nanofluid dispersion stability. The objective of this study is to propose stability diagrams for nanofluid wherein polymeric surfactants were used in the nanofluid at different thermophysical conditions. A molecular dynamic approach is proposed through consideration of different forces to represent conditions wherein such selected nanofluid would be stable through investigation. Hence, an energy approach ~~is~~ was implemented to study the dispersion stability of nanofluid at different thermophysical conditions. Then the stability diagram for alumina-water nanofluid at different conditions ~~are~~ was generated based on the nanofluid characteristics such as nanoparticle diameter, types of polymeric surfactants, fluid temperature and flow field temperature gradient.

FORCES ON THE NANOPARTICLES

Dispersed nanoparticles in a base fluid are affected by different forces. These forces have a particular range of effectiveness and some limitations to act. In addition, the forces between nanoparticles can be attractive or repulsive and may also be short-range or long-range forces (24). These forces are drag, thermophoresis, Brownian, van der Waals and electrical double layer forces. Van der Waals and electrical double layer forces are interparticle forces and the combination of them was introduced as DLVO theory (25). Figure 1 shows schematically DLVO potential energy between two particles.

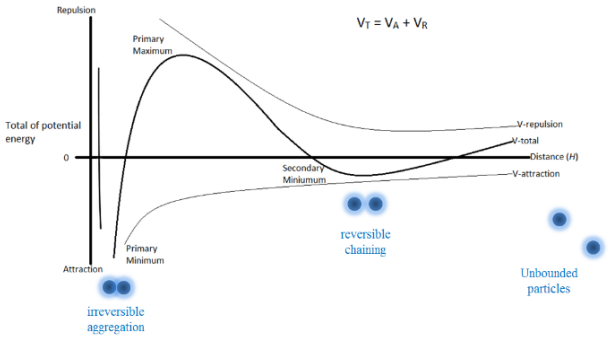

Fig.1. DLVO potential energy between nanoparticles

Recommended correlation for DLVO potential energy is given by (26)

$$E_{DLVO} = \pi\varepsilon\varepsilon_0 d_p \psi_0^2 e^{-k(L-x(t))} - \frac{Ad_P}{24(L-x(t))} \quad (1)$$

Where k is the inverse of Debye length ($k = 3.29 \times \sqrt{[c]}(\mathrm{nm}^{-1})$), [c] is the molar concentration of monovalent electrolyte and ε_0 is the permittivity of free space ($\varepsilon_0 = 8.854 \times 10^{-12} \frac{c^2}{\frac{J}{m}}$).

Other forces are hydrodynamic forces acting on each particle individually. These forces can be defined mathematically as follows:

Drag force

The recommended correlation for drag force, is given by (26)

$$F_D = \frac{18\mu}{\rho_P d_P^2} \times \frac{C_D Re}{24} \times (V_1 - V_2) \times m_P \quad (2)$$

Here V_p is the particle velocity, V_1 the fluid velocity, m_p nanoparticle mass, c_D the drag coefficient, ρ_p the density of nanoparticle, μ the dynamic viscosity of base fluid, and d_p the particle diameter. Re is the relative Reynolds number, given by:

$$Re = \frac{\rho d_p |V_p - V_1|}{\mu} \quad (3)$$

There are various models of the drag coefficient C_D for nanoparticles. Among them Stoke's law seems to be appropriate (27):

$$F_D = \frac{18\mu}{\rho_P d_P^2 C_c} \times (V_1 - V_2) \times m_P \quad (4)$$

Where C_C is the Cunningham correction factor for Stoke's drag force, is given by

$$C_c = 1 + \frac{2\lambda}{d_P}\left(1.257 + 0.4e^{-\left(\frac{1.1 d_P}{2\lambda}\right)}\right) \quad (5)$$

λ is the molecular mean free path.

Brownian force

Recommended correlation for Brownian force, is given by: (28)

$$F_B = m_P \times \zeta \sqrt{\frac{\pi s_0}{\Delta t}} \quad , \quad s_0 = \frac{216\upsilon k_B T}{\pi^2 \rho d_P \left(\frac{\rho_P}{\rho}\right)^2 C_c} \quad (6)$$

Where ζ is a Gaussian random number between zero and one. For simplicity $\zeta = 0.5$ is considered. The Brownian force arises as a result of the collisions of molecules with the particles and acts in a time corresponding to the time of contact during a collision (~ picoseconds). Thus, for such a time interval, drag force is considered constant and Stoke's correlation is acceptable. (28)

Thermophoresis force

Nanoparticles suspended in a base fluid with a temperature gradient experience a force in the direction opposite to that of the temperature gradient. This phenomenon is known as thermophoresis.

Historically, there had been three theoretical approaches in thermophoresis studies that correspond to the Knudsen number range including the free molecule regime, near continuum regime and transition regime. However, the corresponding equations are derived for the suspension of solid particles in ideal gases.

A modification may be necessary to use them for solid–liquid suspensions (nanofluids) (29). As it is known, water molecules are linked to ~~with~~ each other by hydrogen bonds which have a length of three Angstroms at maximum and an average length of about 1.9 Angstroms.

Hence, the free molecule length for water molecules is of order 10^{-11}(m). On the other hand, the characteristic length of a water molecule (diameter of a water molecule) is about two Angstroms and then the Knudsen number is:

$$k_n = \lambda/a \rightarrow \quad k_n = \frac{10^{-11}}{2\times10^{-10}} \cong 0.05 \tag{7}$$

Where a is the characteristic length of a water molecule and λ is the molecular mean free path. Since the Knudsen number is very small ($k_n \ll 1$) and the contents are liquid instead of gas, a correlation corresponding to the near continuum regime for liquid nanofluid could be used. This in non-dimensional form is: (29)

$$F_T = \frac{24\pi}{5} \times \frac{c_{tc}k_n(k_{21}+c_tk_n)}{(1+3c_mk_n)(1+2k_{21}+2c_tk_n)} \tag{8}$$

Where k_{21}, is given by:

$$k_{21} = k_f/k_p \tag{9}$$

However, the dimensional form of this correlation i:s (26)

$$F_T = \frac{6\pi\mu^2 d_p c_s(k_r+c_tk_n)}{\rho(1+3c_mk_n)(1+2k_r+2c_tk_n)} \times \frac{1}{T} \times \frac{\partial T}{\partial x} \tag{10}$$

Where $k_r = k_f/k_p$, $c_s = 1.17$, $c_m = 1.14$, and $c_t = 2.18$.

THE COLLISION ANALYSIS OF COVERED PARTICLES WITH A POLYMER

Regarding the polymer-coated nanoparticles, it was found that the density of the polymer is a specific amount around a particle. While two polymer-coated particles collide with each other, the density will increase and cause a steric force. It can be generally said that there are two types of collisions for polymer-coated particles.

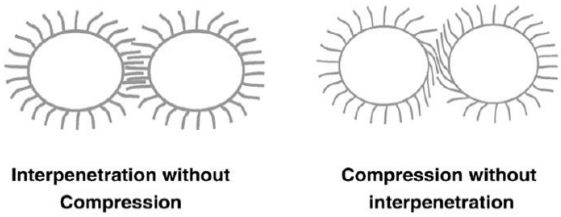

Fig. 2. Different types of collision between two polymer-coated particles

A) In the case of a perfectly elastic collision, the polymer layer may undergo some compression and the polymer chains do not overlap each other. This case has a low probability.

B) In this more common case of collision, the polymer~~s~~ chains may overlap with each other and the density of the polymer layer increases in the overlapping region. These are schematically illustrated in Fig.2. In both cases, due to an increase in the density of the polymer layer between the two particles, osmotic pressure difference will emerge which causes the creation of a force between the two particles.

C) In this more common case of collision, the polymer~~s~~ chains may overlap with each other and the density of the polymer layer increases in the overlapping region. These are schematically illustrated in Fig.2. In both cases, due to an increase in the density of the polymer layer between the two particles, osmotic pressure difference will emerge which causes the creation of a force between the two particles.

In the first case (case A), besides a driving force due to the difference in osmotic pressure, an elastic force will emerge~~d~~ that will separate the particles from each other (30). However, when the particles are sufficiently close to each other, the elastic force appears for the second case (case B). In a real situation a combination of both A and B cases may occur. Hence, can be concluded that the local monomeric density increases in the collision area and this leads to the formation of a powerful force. This force is formed due to an increase in the osmotic pressure of the collision area which can be a repulsive or attractive force depending on the amount of the Flory-Huggins number (χ).

MATHEMATICAL FORMULATION

It is assumed that all particles are completely coated with the polymers and the radius of the polymer layer around a nanoparticle is equal to L_s (see Fig.3).

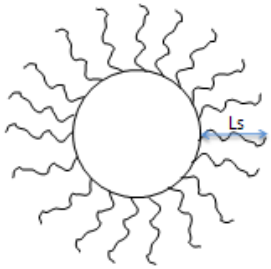

Fig. 3. Schematic of polymer layer around nano particle

In this case, the radius of the polymer around the nanoparticle obtained from the following equation (30):

$$L_s(nm) = 0.06\ (M_w)^{0.5} \tag{11}$$

Where M_w is the molecular weight of the polymer. Considering particles 1 and 2 in Fig. 4, DLVO force will not count for particle 2 in respect to the other forces acting on this particle, the velocity distribution of the particle exists at different points. Using the velocity distribution, its kinetic energy can be calculated at different locations.

The kinetic energy is as a result of the exerted forces on the particle (except that steric force and DLVO) which is transferred to the particle.

On the other hand, the potential energy between two particles is available in respect of the existing relations. Now, it can be checked whether the transferred kinetic energy to the particle can overcome the potential energy barrier of the steric and DLVO or not.

In this regard, the parameters will be changed for different values to see how the kinetic energy of the particle will prevail on the total energy of the steric and DLVO. The analysis is named as the "two particles method":

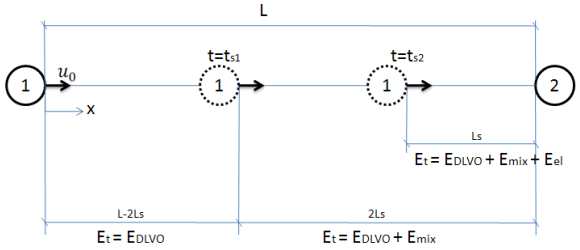

Fig. 4. Different regions in the collision path of polymer-coated particles

In Fig.4, t_{s1} is the elapsed time of particle 1 to reach where particle 2 has a distance equal to $2L_s$ (the extent of the polymer layers overlaps around nanoparticles). t_{s2} represents the time of particle 1 reaching a position in which particle 2 has a distance equal to L_s (the collision moment of the polymer layer around particle 1 to the surface of the particle 2).

It can be said that as long as the polymer layer interaction has not been formed ($t < t_{s1}$), the potential energy between the two particles can be calculated only from the equation of the DLVO potential energy (30).

$$E_t = E_{DLVO} = \pi\varepsilon\varepsilon_0 d_p \psi_0^2 e^{-k(L-x)} - \frac{Ad_p}{24(L-x)} \tag{12}$$

For the time it takes from the beginning of the polymer layers overlap to contact between the polymer layers and the particle's surface ($t_{s1} < t < t_{s2}$), the potential energy between the two particles is equal to the total DLVO potential energy and the resulted energy from the polymer layers' interaction (30).

$$E_{mix} = \frac{16\pi d_P k_B T}{SV}\frac{V_t^2}{L_s^4}\left(\frac{1}{2}-x\right)\left(L_s-\frac{L-x}{2}\right)^6 \tag{13}$$

$$E_t = E_{DLVO} + E_{mix} = \pi\varepsilon\varepsilon_0 d_p \psi_0^2 e^{-k(L-x)} - \frac{Ad_p}{24(L-x)} + \frac{16\pi d_P k_B T}{SV}\frac{V_t^2}{L_s^4}\left(\frac{1}{2}-x\right)\left(L_s-\frac{L-x}{2}\right)^6 \tag{14}$$

Where, V_f represents the mean-volume-fraction of monomers in the polymer layer around a nanoparticle, v is the molecular volume of the base fluid and χ is the Flory-Huggins number.

Finally, for the time it takes from the contact of the polymer layer to completely agglomerate the particles together (t_{s2} <t), the equation of the potential energy between the particles is as follow (30):

$$E_{mix} = \frac{2\pi d_P k_B T}{V} V_f^2 \left(\frac{1}{2}-x\right)\left(\frac{L-x}{2L_s}-\frac{1}{4}-\ln\frac{L-x}{L_s}\right) \tag{15}$$

$$E_{el} = \frac{\pi d_P k_B T L_s^2 \rho_{Poly}}{M_w} V_f^2 \left\{\frac{L-x}{L_s}\ln\left[\frac{L-x}{L_s}\left(\frac{3-\frac{L-x}{L_s}}{2}\right)^2\right] - 6\ln\left(\frac{3-\frac{L-x}{L_s}}{2}\right) + 3\left(1-\frac{L-x}{L_s}\right)\right\} \tag{16}$$

$$E_t = E_{DLVO} + E_{mix} + E_{el} = \pi\varepsilon\varepsilon_0 d_p \psi_0^2 e^{-k(L-x)} - \frac{Ad_p}{24(L-x)} + \frac{2\pi d_P k_B T}{V} V_f^2 \left(\frac{1}{2}-x\right)\left(\frac{L-x}{2L_s}-\frac{1}{4}-\ln\frac{L-x}{L_s}\right) + \frac{\pi d_P k_B T L_s^2 \rho_{Poly}}{M_w} V_f^2 \left\{\frac{L-x}{L_s}\ln\left[\frac{L-x}{L_s}\left(\frac{3-\frac{L-x}{L_s}}{2}\right)^2\right] - 6\ln\left(\frac{3-\frac{L-x}{L_s}}{2}\right) + 3\left(1-\frac{L-x}{L_s}\right)\right\} \tag{17}$$

Where, E_{el} represents the energy of an elastic collision of the polymer layer with the particle's surface, ρ_{poly} is the polymer density and M_w is the molecular weight of the polymer.

Now, using Newton's second law for a particle motion, and considering equations (4, 6 and 10), the velocity and displacement of the particle can be determined by the following equations respectively (in equations, fluid is static and V_1=0):

$$V_p(t) = (u_0 - \frac{A_1+B}{C})\, e^{-Ct} + \frac{A_1+B}{C} \tag{18}$$

$$x(t) = (u_0 - \frac{A_1+B}{C}) \times \frac{-e^{-Ct}}{C} + \frac{A_1+B}{C} \times t + (\frac{u_0}{C} - \frac{A_1+B}{C^2}) \tag{19}$$

Where:

$$A_1 = \frac{1}{m_p} \times \frac{6\,\pi\mu^2 d_p\, c_s(\,k_r + c_t k_n)}{\rho(1+3\,c_m k_n)\,(1+2\,k_r + 2c_t k_n)} \times \frac{1}{T} \times \frac{\partial T}{\partial x}$$

$$B = \zeta\sqrt{\frac{\pi s_0}{\Delta_t}}$$

$$C = \frac{18\mu}{\rho_p {d_p}^2 c_c}$$

The initial velocity of the nanoparticles, u_0, is calculated by (31):

$$u_0 = \sqrt{\frac{3k_B T}{m_P}} \tag{20}$$

The kinetic energy of the particle and its total potential energy are determined in a very small-time interval. Then a comparison between them is performed.

$$\text{Kinetic energy} = K = \frac{1}{2} m_p V_p(t)^2 = \frac{1}{2} m_p ((u_0 - \frac{A_1+B}{C})\, e^{-Ct} + \frac{A_1+B}{C})^2 \tag{21}$$

If the magnitude of E_t is larger than the kinetic energy of the particle in a specific time, it could be said that the nanofluid is stable in such a condition. With changing the thermo-fluid conditions, the stability could also change and then a "stability diagram" could be obtained.

RESULTS AND DISCUSSION

The results here are based on the force analysis presented earlier. The stability diagram of the water-alumina oxide nanofluid is presented in different temperature gradients and working fluid temperatures for various nanoparticle diameters. The PAA[1] and PMAA[2] surfactants are considered as surfactant of the stability of the nanofluid.

The stability diagram for alumina-water nanofluid with volume fraction of 0.01, PH=7, while no surfactant is added, is represented in Fig.5. As can be seen, increasing the temperature gradient as well as the working fluid temperature, smaller nanoparticles are needed to have a stable nanofluid.

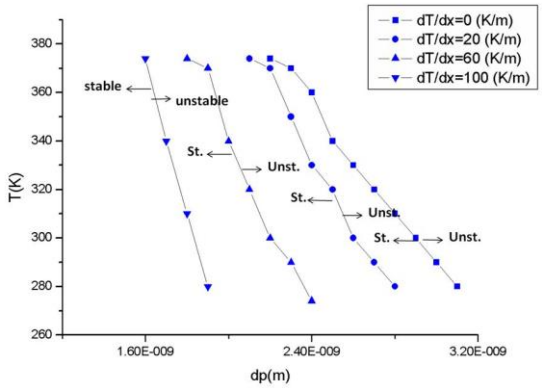

Fig. 5. stability diagram of Al_2O_3-water nanofluid without surfactant

It is shown that without using surfactant very fine nanoparticles are required (smaller than 4nm) to be sure of the Physico-chemical stability of the nanofluid at different thermo-fluid conditions.

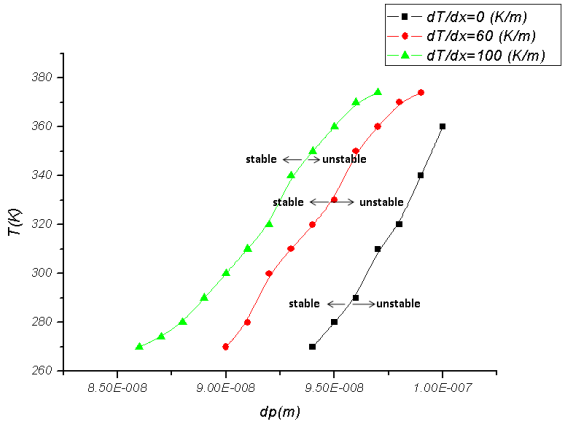

Fig. 6. stability diagram of Al_2O_3-water nanofluid with PMAA surfactant

To show the effect of using a PMAA surfactant on the stability diagram of Al_2O_3-water nanofluid, Fig. 6 is presented. As shown, using the PMAA polymer causes achievement of the stability conditions for larger nanoparticle with a mean diameter of i.e., 85nm (compared to no surfactant nanofluid). It is interesting to note that the stability zone expanded to the higher nanoparticle mean diameter through increasing the working fluid temperature. Through increasing the temperature, the PMAA solubility increases and therefore polymer chains expand, increasing the range of the steric force and consequently, the potential energy among the particles is strengthened.

[1] Poly acrylic acid
[2] Poly methacrylic acid

So that's across specific temperature, increase of the steric energy reinforces the potential energy between the particles and causes the kinetic energy of particles unable to overcome it, stabilizing the nano-fluid. However, by increasing the temperature gradient in the nanofluid, the kinetic energy of the particle increases due to the creation and strengthening of the thermophoresis force; therefore, the unstable area becomes larger and smaller nanoparticles are required to have a stable nanofluid.

To see the effect of another surfactant (PAA) in the nanofluid stability, Fig. 7 is presented. As seen, using a PAA polymer, variations compared to using PMAA is obvious. For a given temperature gradient, increasing the working fluid temperature required smaller nanoparticles diameters for a stable nanofluid. This is because of the solubility reduction of the polymer due to the extremely low solubility of the base fluid at low temperatures.

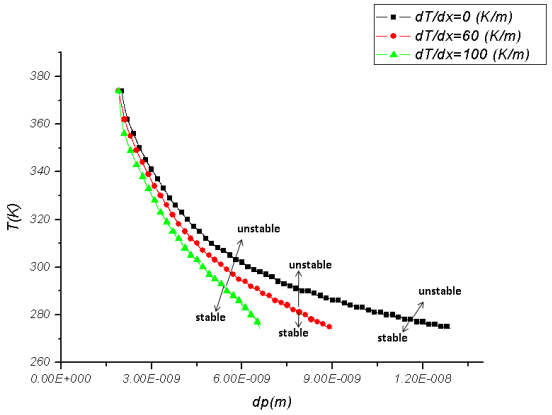

Fig. 7. stability diagram of Al_2O_3-water nanofluid with PAA surfactant

Polymers around the particles are very dense and diffusion of the polymer layers into each other is more difficult, hence the elastic force is reinforced among the particles. Since the kinetic energy of the nanoparticles is low at this temperature, the energy content of the nanoparticles cannot overcome the steric force, and the nanofluid will be stable. However, by increasing the working fluid temperature, the kinetic energy of nanoparticles and the diameter of polymer layer increase, and therefore the density of the polymer layer decreases. In this regard, the polymer around the two particles can better penetrate each other. With a further increase in temperature, the kinetic energy overcomes the steric force, and thus the nanofluid becomes unstable. As seen in the previous case, increasing the temperature gradient also increases the kinetic energy of the particle and the unstable area becomes larger. It also is observed that due to the small size of the PAA polymer, the diameter of the formed polymer layer around the particles (in comparison with PMAA) is small and can only provide the stability for the nanofluid up to around 13.2 nm diameter.

CONCLUSION

Based on a molecular dynamic approach, stability diagrams of AL_2O_3-water nanofluid are presented. Forces, including attractive and repulsive forces such as drag, thermophoresis, Brownian, van der Waals and electrical double layer forces were considered. Additionally, the steric repulsion arising from using a surfactant for stabilizing the nanofluid, is taken into account. For different nanoparticle mean diameters, working fluid temperature and temperature gradient, the stability diagram of nanofluid is introduced. Two different surfactants including PMAA and PAA were considered. Because of the different effects of these surfactants the results are different. It is shown that using a PMAA surfactant establishes a stable nanofluid with a large nanoparticle diameter (about 80nm) compared to nanofluid without a surfactant. However, the effect of PAA in this regard is less important. In the case of using PAA for a given temperature gradient, increasing the working fluid temperature required smaller nanoparticle diameters to result in a stable nanofluid.

In the case of PMAA for a given temperature gradient, a stable nanofluid can be achieved with larger nanoparticle diameters while increasing the working fluid temperature.

REFERENCES

[1] Hunt AJ. Energy USDo, Energy LBL, Division E. Small particle heat exchangers: Department of Energy, Lawrence Berkeley Laboratory, Energy and Environment Division; 1978.

[2] Lenert A. Nanofluid-based Receivers for High-Temperature, High-flux Direct Solar Collectors: Massachusetts Institute of Technology; 2010.

[3] Abdelrahman M, Fumeaux P, Suter P. Study of solid-gas-suspensions used for direct absorption of concentrated solar radiation. Solar Energy. 1979; 22(1): 45-48.

[4] Drotning WD. Optical properties of solar-absorbing oxide particles suspended in a molten salt heat transfer fluid. Solar Energy. 1978; 20(4): 313-319.

[5] Kumar S, Tien C. Analysis of combined radiation and convection in a particulate-laden liquid film. Journal of Solar Energy Engineering. 1990; 112(4): 293-300.

[6] Lenert A, Wang EN. Optimization of nanofluid volumetric receivers for solar thermal energy conversion. Solar Energy. 2012; 86(1): 253-265.

[7] Tyagi H, Phelan P, Prasher R. Predicted Efficiency of a Low-Temperature Nanofluid-Based Direct Absorption Solar Collector. Journal of Solar Energy Engineering. 2009; 131(4): 041004.

[8] Khullar V, Tyagi H, Phelan PE, Otanicar TP, Singh H, Taylor RA. Solar Energy Harvesting Using Nanofluids-Based Concentrating Solar Collector. Journal of Nanotechnology in Engineering and Medicine. 2013; 3(3): 031003.

[9] Otanicar TP, Phelan PE, Golden JS. Optical properties of liquids for direct absorption solar thermal energy systems. Solar Energy. 2009; 83(7): 969-977.

[10] Otanicar TP, Phelan PE, Prasher RS, Rosengarten G, Taylor RA. Nanofluid-based direct absorption solar collector. Journal of Renewable and Sustainable Energy. 2010; 2: 033102.

[11] Taylor R, Phelan P, Otanicar T, Adrian R, Prasher R. Nanofluid optical property characterization: towards efficient direct absorption solar collectors. Nanoscale Research Letters. 2011; 6(1): 1-11.

[12] Taylor RA, Phelan PE, Otanicar TP, Walker CA, Nguyen M, Trimble S, et al. Applicability of nanofluids in high flux solar collectors. Journal of Renewable and Sustainable Energy. 2011; 3(2).

[13] Zhu Q, Cui Y, Mu L, Tang L. Characterization of Thermal Radiative Properties of Nanofluids for Selective Absorption of Solar Radiation. International Journal of Thermophysics. 2013; 34(12): 2307-2321.

[14] Khullar V, Tyagi H, Hordy N, Otanicar TP, Hewakuruppu Y, Modi P, et al. Harvesting solar thermal energy through nanofluid-based volumetric absorption systems. International Journal of Heat and Mass Transfer. 2014; 77(0): 377-384.

[15] Farzaneh H, Behzadmehr A, Yaghoubi M, Samimi A, Sarvari SMH. Stability of nanofluids: Molecular dynamic approach and experimental study. Energy Conversion and Management. 2016; 111: 1-14.

[16] Zareei M, Yoozbashizadeh H, Madaah Hosseini HR. Investigating the effects of pH, surfactant and ionic strength on the stability of alumina/water nanofluids using DLVO theory. Journal of Thermal Analysis and Calorimetry. 2019; 135(2): 1185-1196.

[17] Cacua K, Ordoñez F, Zapata C, Herrera B, Pabón E, Buitrago-Sierra R. Surfactant concentration and pH effects on the zeta potential values of alumina nanofluids to inspect stability. Colloids and Surfaces A: Physicochemical and Engineering Aspects. 2019; 583: 123960.

[18] Ouikhalfan M, Labihi A, Belaqziz M, Chehouani H, Benhamou B, Sarı A, et al. Stability and thermal conductivity enhancement of aqueous nanofluid based on surfactant-modified TiO2. Journal of Dispersion Science and Technology. 2019; 1-9.

[19] Kaggwa A, Carson JK, Atkins M, Walmsley M. The effect of surfactants on viscosity and stability of activated carbon, alumina and copper oxide nanofluids. Materials Today: Proceedings. 2019; 18: 510-519.

[20] Zhai Y, Li L, Wang J, Li Z. Evaluation of surfactant on stability and thermal performance of Al2O3-ethylene glycol (EG) nanofluids. Powder Technology. 2019; 343: 215-224.

[21] Sharaf OZ, Taylor RA, Abu-Nada E. On the colloidal and chemical stability of solar nanofluids: From nanoscale interactions to recent advances. Physics Reports. 2020; 867: 1-84 .

[22] Razavi SR, Sadeghalvaad M, Sabbaghi S. Experimental investigation on the stability and thermophysical properties of Al2O3/DW and CuO/DW nanofluids to be utilized in an indirect water bath heater. Journal of Thermal Analysis and Calorimetry. 2020; 142(6): 2303-2318.

[23] Mukesh Kumar PC, Palanisamy K, Vijayan V. Stability analysis of heat transfer hybrid/water nanofluids. Materials Today: Proceedings. 2020; 21: 708-712.

[24] Goodwin J. Colloids and interfaces with surfactants and polymers: John Wiley & Sons; 2009.

[25] Grodzka J, Pomianowski A. On the necessity of modifying the dlvo theory (in equlibrium systems). Physicochemical Problems of Mineral Processing. 2005; 39: 11-20.

[26] Wen D, Zhang L, He Y. Flow and migration of nanoparticle in a single channel. Heat and mass transfer. 2009; 45(8): 1061-1067.

[27] Das SK, Choi SUS, Yu W, Pradeep T. Convection in Nanofluids. Nanofluids: John Wiley & Sons, Inc.; 2007; 209.

[28] Wang X, Gidwani A, Girshick SL, McMurry PH. Aerodynamic focusing of nanoparticles: II. Numerical simulation of particle motion through aerodynamic lenses. Aerosol science and technology. 2005; 39(7): 624-636.

[29] Zheng F. Thermophoresis of spherical and non-spherical particles: a review of theories and experiments. Advances in colloid and interface science. 2002; 97(1): 255-278.

[30] Lu K. Theoretical analysis of colloidal interaction energy in nanoparticle suspensions. Ceramics International. 2008; 34(6): 1353-1360.

[31] Jiang W, Ding G, Peng H, Hu H. Modeling of nanoparticles' aggregation and sedimentation in nanofluid. Current Applied Physics. 2010; 10(3): 934-941.